Elastic full waveform inversion for near surface imaging in CMP domain

Zhiyang Liu, Jie Zhang, University of Science and Technology of China (USTC)*

Summary

We develop an elastic full waveform inversion method in the CMP domain for near surface imaging. Sometimes, applying acoustic wavefield solution may not be sufficient for near surface imaging on land. On the other hand, performing 2D or 3D elastic waveform inversion in shot domain is highly time-consuming. A practical approach for solving an elastic problem is to conduct 1D inversion in the CMP domain and then interpolate the interval velocities at CMP locations to create a 2D or 3D velocity model. The CMP method assumes small lateral velocity variation in the local area, thus, it may not be suitable for imaging complex structures, yet useful for many land cases. Numerical tests on synthetic and application on field data from an oil field in China produces reliable results.

Introduction

The unprocessed elastic full waveform data is a composition of P-wave, converted waves and surface waves, all of which can be used to provide the near surface structural information. We can use the early arrivals to invert a P-wave velocity model, and then use the surface wave data to invert an S-wave velocity model. Near-surface P- and S-wave velocity models are needed for statics corrections when processing 3C data with converted waves included.

The problems with elastic full waveform inversion were well explored in both 2D and 3D (Tarantola, 1984; Warner et al., 2008). However, when inverting massive seismic data, these methods are not efficient. Therefore, in the seismic industry, a common practice for inverting seismic waveform is to solve an acoustic wavefield problem, especially for marine problems (Prieux et al., 2010). For land imaging, however, acoustic assumption is often insufficient. Therefore, we look into the problem of the elastic full waveform inversion, but in the CMP domain, and invert a 1D velocity structure for each CMP gather. The approach takes only 8 minutes for one inversion iteration of a CMP gather on a single CPU. We shall describe the method in the following.

Elastic waveform inversion in CMP domain

s In the case of elastic problem in the CMP domain, our approach computes theoretical seismograms from a point source in a layered medium by using the frequency-wavenumber (F-K) integration method for the forward modeling (Zhu and Rivera, 2002). One forward modeling takes about 50s in average on a single CPU.

In the inversion process for the synthetic model, we build a ten-layer over half-a-space near-surface model and 15 CMP gathers. Then, we use the early arrivals to invert a P-wave velocity model, and use the surface wave data to invert an S-wave velocity model. Also, attenuation is taken into account during the elastic waveform inversion. Figures 1 and 2 show the synthetic inversion of the P-wave and S-wave velocity models respectively.

(a) The RMS misfit of early arrival waveform inversion

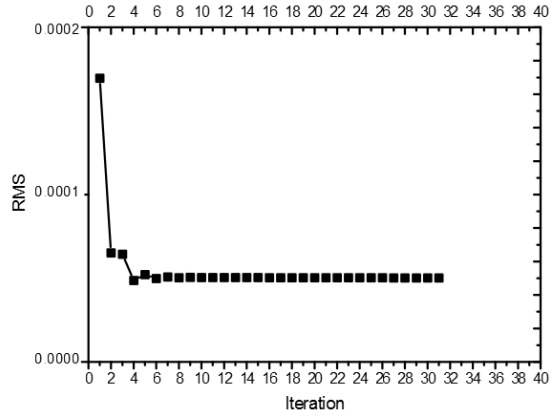

(b) The early-arrival waveform fit of 15 CMP gathers

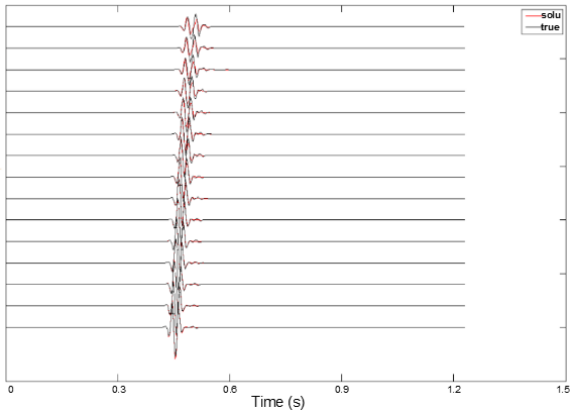

DOI http://dx.doi.org/10.1190/segam2013-1066.1

(c) The near-offset trace fit for early arrivals

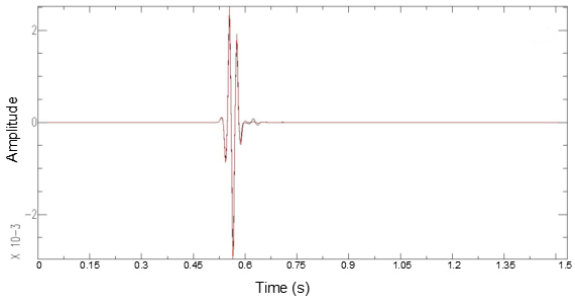

(d) The P-wave velocity model inversion results

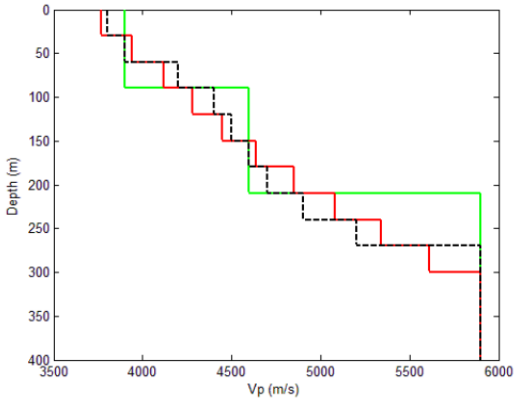

Figure 1: (a) The RMS data chart showing the changes of each iteration; (b) 15 CMP-gather inversion solution (red) and the true data (black) of the synthetic test; (c) Showing the near-offset gather of the inversion solution (red) and the true data (black) of the synthetic test; (d) The P-wave velocity model inversion results where black dotted line represents the true model, green line represents the initial model and red line represents a 1D waveform inversion result.

(a) The RMS misfit of surface-wave waveform inversion

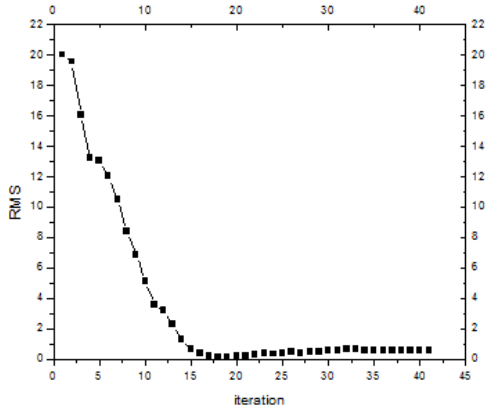

(b) The surface-wave waveform fit of 15 CMP gathers

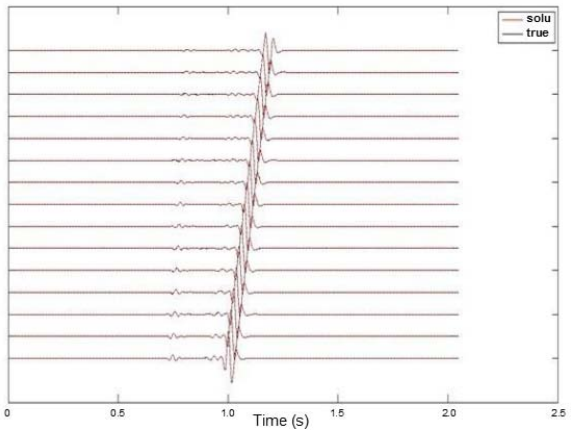

(c) The near-offset waveform fit for surface wave

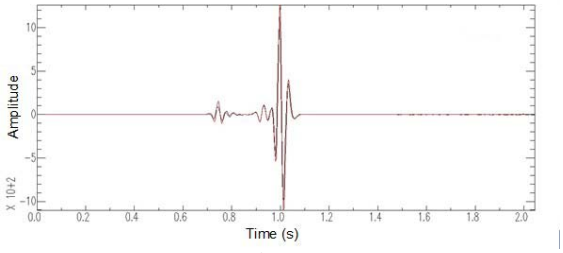

(d) The S-wave velocity model from inversion

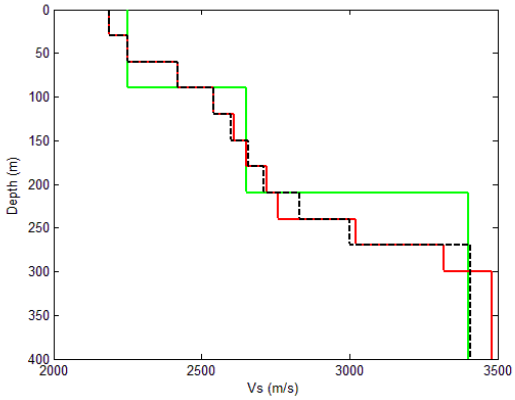

Figure 2: (a) The RMS data chart showing the changes of each iteration; (b) 15 CMP-gather inversion solution (red) and the true data (black) of the synthetic test; (c) Showing the near-offset waveform fit after inversion: synthetics (red) and input data (black); (d) The S-wave velocity model from inversion,where black dotted line represents the true model, green line represents the initial model and red line represents a 1D waveform inversion result.

Real data applications

a Having demonstrated that the elastic waveform inversion is viable in CMP domain, we apply the above method to real data from an oil field in China. The survey is

DOI http://dx.doi.org/10.1190/segam2013-1066.1

performed in an area where the subsurface structures are predominantly layered. We first perform the first-arrival traveltime tomography, and resolve a near-surface P-wave velocity model as shown in Figure 3.

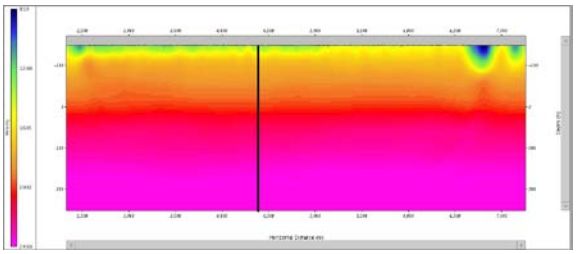

Figure 3: Traveltime tomographic solution using data from an oil field in China. We choose the CMP point at the black line to apply elastic waveform inversion.

In our particular implementation, we select a single CMP gather from the 2D line (Figure 4), which was acquired in an oil field where swampland is known to exist. And then, we normalized amplitudes and matched the source spectrum to the field data.

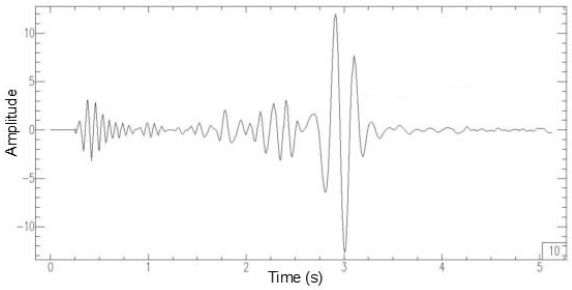

Figure 4: A trace for elastic waveform inversion.

Figures 5 and 6 show the inversion results of the P-wave and S-wave velocity models respectively in the top few hundred meters of the subsurface. Interestingly the gather appear as low-velocity features for P-wave and S-wave at the top of the layers; we also see this in the traveltime tomographic solution. In addition, we notice that there is a significant change in Vp/Vs within this gather, which confirms that the area is swampy. Also, the computation time of P-wave and S-wave inversion is of 7 minutes 50 seconds and 8 minutes respectively.

(a) Comparison among initial data, solution and true data

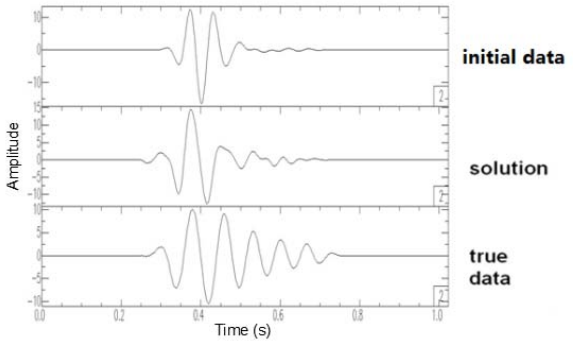

(b) The solution of a single CMP gather for early arrivals

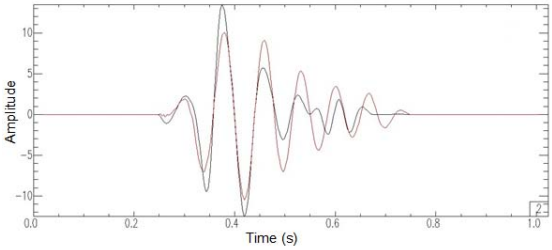

(c) The P-wave velocity model from inversion

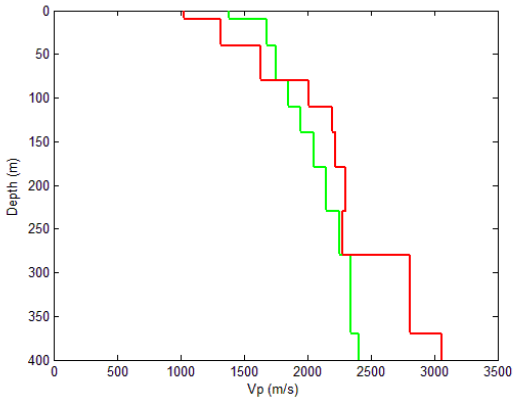

Figure 5: (a) The comparison among initial synthetics, solution and true data; (b) Showing the single-gather inversion solution (red) and the true data (black); (c) The P-wave velocity models where green line represents the initial model and red line represents the final solution.

DOI http://dx.doi.org/10.1190/segam2013-1066.1

(a) Comparison among initial data, solution and true data

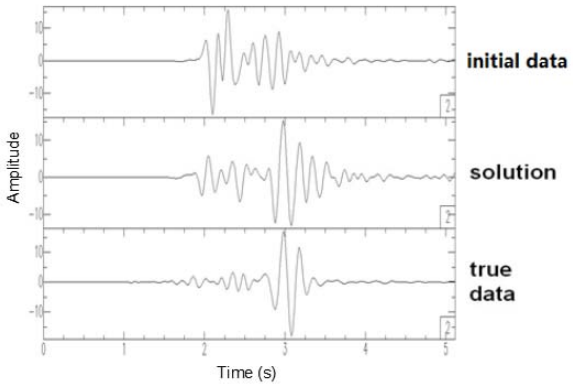

(b) Waveform fit for S-wave velocity inversion

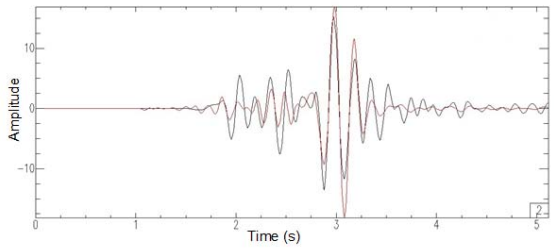

(c) The S-wave velocity inversion model result

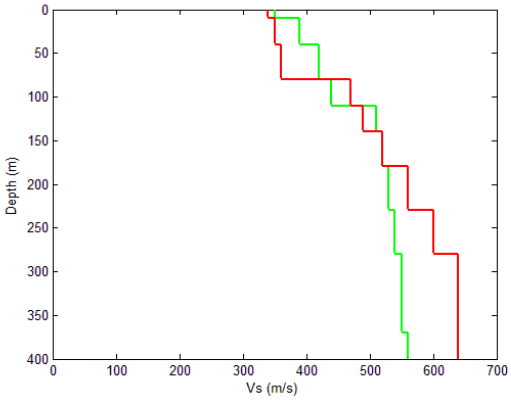

Figure 6: (a) The comparison among initial data, solution and input data; (b) Showing waveform fit with synthetics (red) and the input data (black); (c) The S-wave velocity inversion model result where green line represents the initial model and red line represents a 1D waveform inversion result.

Conclusions

We develop an elastic waveform inversion technique in the CMP domain. We demonstrate that this approach is efficient for deriving meaningful high-resolution elastic parameters in the CMP domain compared to that of 2D or 3D in the shot domain. The numerical tests and application on real data further show the possible applicability of our approach for solving an elastic problem.

Acknowledgments

We appreciate the support from GeoTomo, allowing us to use TomoPlus software package to help perform this study.

DOI http://dx.doi.org/10.1190/segam2013-1066.1

http://dx.doi.org/10.1190/segam2013-1066.1

EDITED REFERENCES

Note: This reference list is a copy-edited version of the reference list submitted by the author. Reference lists for the 2013 SEG Technical Program Expanded Abstracts have been copy edited so that references provided with the online metadata for each paper will achieve a high degree of linking to cited sources that appear on the Web.

REFERENCES

Berteussen, K. A., 1977, Moho depth determinations based on spectral ratio analysis of NORSAR long-period P waves: Physics of the Earth and Planetary Interiors, **31**, 313–326.

Constable, S. C., R. L. Parker, and C. G. Constable, 1987, Occam's inversion: A practical algorithm for generating smooth models from electromagnetic sounding data: Geophysics, **52**, 289–300.

Prieux, V., R. Brossier, J. H. Kommendal, O. I. Barkved, S. Operto, and J. Virieux, 2010, Application of 2D acoustic frequency-domain full-waveform inversion to OBC wide-aperture data from the Valhall field: Presented at the 80th Annual International Meeting, SEG.

Shaw, P. R., and J. A. Orcutt, 1985, Waveform inversion of seismic refraction data and applications to young Pacific crust: Geophysical Journal International, **82**, 375–414.

Tarantola, A., 1984, Inversion of seismic-reflection data in the acoustic approximation: Geophysics, **49**, 1259–1266.

Wang, C. Y., and R. B. Herrmann, 1980, A numerical study of P, SV, and SH-wave generation in a plane layered medium: Bulletin of the Seismological Society of America, **70**, 1015–1036.

Warner, M., I. Stekl, and A. Umpleby, 2008, 3D wavefield tomography: Synthetic and field data examples: Presented at the 78th Annual International Meeting, SEG.

Zhu, L., and L. A. Rivera, 2002, A note on the dynamic and static displacements from a point source in multilayered media: Geophysical Journal International, **148**, 619–627.